The Journal of Immunology

Therapeutic Potential of Mesenchymal Cell–Derived miRNA-150-5p–Expressing Exosomes in Rheumatoid Arthritis Mediated by the Modulation of MMP14 and VEGF

Zhe Chen, Hanqi Wang, Yang Xia, Fuhua Yan and Yong Lu

J Immunol 2018; 201:2472-2482; Prepublished online 17 September 2018;
doi: 10.4049/jimmunol.1800304
http://www.jimmunol.org/content/201/8/2472

The Journal of Immunology is published twice each month by
The American Association of Immunologists, Inc.,
1451 Rockville Pike, Suite 650, Rockville, MD 20852

Print ISSN: 0022-1767 Online ISSN: 1550-6606.

Therapeutic Potential of Mesenchymal Cell–Derived miRNA-150-5p–Expressing Exosomes in Rheumatoid Arthritis Mediated by the Modulation of MMP14 and VEGF

Zhe Chen,*[,1] Hanqi Wang,*[,1] Yang Xia,[†] Fuhua Yan,* and Yong Lu*

Rheumatoid arthritis (RA) is a chronic autoimmune disease characterized by synovial tissue inflammation and joint destruction associated with the activation of angiogenesis. Exosomes, which play a role in cell-to-cell communication as carriers of genetic information, transfer microRNAs (miRNAs or miRs) between cells and have been studied as delivery vehicles for therapeutic molecules. The aim of the current study was to investigate the therapeutic effect of mesenchymal stem cell (MSC)–derived miR-150-5p exosomes on joint destruction in RA. The expression and secretion of miR-150-5p, matrix metalloproteinase (MMP) 14, and vascular endothelial growth factor (VEGF) in RA patients and fibroblast-like synoviocytes (FLS) were examined by quantitative RT-PCR, ELISA, and Western blotting. Immunohistochemistry was used to assess angiogenesis. MSCs were transfected with an miR-150-5p expression plasmid, and MSC-derived exosomes were harvested. The effect of MSC-derived miR-150-5p exosomes (Exo-150) on MMP14 and VEGF expression was examined. The effects of Exo-150 on cell migration and invasion in cytokine-stimulated FLS from RA patients were examined by HUVEC tube formation and transwell assays. The effect of Exo-150 in vivo was examined in a collagen-induced arthritis mouse model. Exo-150 decreased migration and invasion in RA FLS and downregulated tube formation in HUVECs by targeting MMP14 and VEGF. Injection of Exo-150 reduced hind paw thickness and the clinical arthritic scores in collagen-induced arthritis mice. Exo-150 reduced joint destruction by inhibiting synoviocyte hyperplasia and angiogenesis. Exosomes facilitate the direct intracellular transfer of miRNAs between cells and represent a potential therapeutic strategy for RA. ***The Journal of Immunology*****, 2018, 201: 2472–2482.**

Rheumatoid arthritis (RA) is a chronic inflammatory disease characterized by leukocyte infiltration into joints, leading to the production of inflammatory mediators and cartilage and bone destruction (1). The inflamed synovium in RA becomes locally invasive and penetrates the surface of cartilage by degrading the extracellular matrix. This degradation is mediated by increased activity of matrix metalloproteinases (MMPs), and MMP-mediated cartilage damage is irreversible, suggesting that the activity of MMPs is a critical step in joint damage (2). The synovium in RA contains fibroblast-like synoviocytes (FLS), which produce MMPs that degrade type II collagen. Membrane type 1 MMP (MT1-MMP or MMP14) is a type I transmembrane proteinase that is expressed on the cell surface and is highly expressed in FLS in the joints of patients with RA (3, 4). MMP14 promotes the invasion of FLS into cartilage and is considered a key enzyme mediating cartilage invasion in RA. In addition, the inflammatory state in RA is maintained by the transport of inflammatory cells to the joints through the activation of angiogenesis (5). Among angiogenic factors, vascular endothelial growth factor (VEGF) and hypoxia-inducible factor 1α (HIF-1α) are crucial as positive regulators of angiogenesis. Targeting angiogenesis has been explored as a therapeutic strategy for the treatment of RA, and several agents that inhibit VEGF production are used as antirheumatic drugs (6).

MicroRNAs (miRNAs or miRs) are small noncoding RNAs that bind to complementary sequences in the 3′ untranslated region (3′-UTR) of target mRNAs, promoting translational repression or target degradation (7, 8). miRNAs regulate many physiological processes, and aberrant expression of certain miRNAs is associated with several human diseases, underscoring their role in disease pathogenesis and their potential as biomarkers and therapeutic targets (9). Dysregulation of miRNAs in synovial fibroblasts, osteoclasts, and T lymphocytes, which mediate joint destruction, causes inflammation and degradation of the extracellular matrix and modulates the invasive behavior of cells (10–13). In addition, altered expression of miRNAs is associated with RA (14, 15).

Despite the potential of miRNAs as therapeutic agents, an effective method for their delivery to the target tissues is required. Exosomes, which are small extracellular vesicles that promote intercellular communication by transferring molecules between cells, have gained increasing interest as delivery vehicles for the transfer of miRNAs (16–18). Exosomes are produced by many types of cells, including reticulocytes, epithelial cells, neurons, and tumor cells; they are secreted and enter the circulatory system, affecting biological processes by delivering their content to target

*Department of Radiology, Ruijin Hospital, Shanghai Jiao Tong University School of Medicine, Shanghai 200025, China; and [†]Department of Physics, Oakland University, Rochester, MI 48309

[1]Z.C. and H.W. contributed equally to this work.

ORCID: 0000-0003-4653-1862 (Y.X.).

Received for publication March 6, 2018. Accepted for publication August 13, 2018.

This work was supported by the National Natural Science Foundation of China (Grant 81372000), the Shanghai Jiao Tong University "Medical-Engineering Cross Fund" (Grant YG2013MS25), the Magnetic Resonance–Dominated Joint Replacement Imaging Evaluation System Research and Clinical Application (Grant 17411964900), and the Action Plan of Major Diseases Prevention and Treatment (Grant 2017ZX01001-S12).

Address correspondence and reprint requests to Prof. Yong Lu, Ruijin Hospital, 197 Ruijin Er Road, Shanghai 200025, China. E-mail address: 18917762053@163.com

The online version of this article contains supplemental material.

Abbreviations used in this article: CIA, collagen-induced arthritis; Exo-67, cel-miR-67–transfected exosome; Exo-150, MSC-derived miR-150-5p exosome; FCM, flow cytometry; FLS, fibroblast-like synoviocyte; HCC, hepatocellular carcinoma; miR/miRNA, microRNA; MMP, matrix metalloproteinase; MSC, mesenchymal stem cell; OA, osteoarthritis; qRT-PCR, quantitative RT-PCR; RA, rheumatoid arthritis; TEM, transmission electron microscope; 3′-UTR, 3′ untranslated region; VEGF, vascular endothelial growth factor.

cells (17). Because miRNAs exist in exosomes, these vesicles can be engineered to deliver miRNAs to target cells (19). Exosomes have several advantages, such as the fact that they do not elicit immune responses, and they can be isolated from mesenchymal stem cells (MSCs), which produce abundant amounts of exosomes (20). MSC-derived exosomes have been reported to exert beneficial effects against myocardial ischemia/reperfusion injury, limb ischemia, graft-versus-host disease, and renal injury and to improve wound healing, promote hepatic regeneration, and improve cartilage and bone regeneration (21–28).

In the current study, we generated miR-150-5p–expressing MSCs and examined the effect of MSC-derived miR-150-5p exosomes (Exo-150) on the expression of MMP14, VEGF secretion, FLS migration and invasion, and angiogenesis in vitro. In addition, we established a mouse model of collagen-induced arthritis (CIA) and examined the effect of Exo-150 in vivo.

Materials and Methods

Ethics statement

All experimental methods in the current study were approved by the research committee at Medical College of Shanghai Jiao Tong University. All experiments were performed in accordance with guidelines from the research committee at the Medical College of Shanghai Jiao Tong University. All experiments using mice were approved by the Institutional Animal Care and Use Committee at Shanghai Jiao Tong University (Animal Welfare Assurance). Surgeries were performed in accordance with the Principles of Laboratory Care and were supervised by a qualified veterinarian.

Collection of human synovial tissue

Serum and synovial tissues were obtained from 11 patients with RA who underwent synovectomy or joint replacement. For comparative analysis, samples of synovium were also obtained from 11 patients with osteoarthritis (OA). All patients provided informed consent to participate in the study. RA was diagnosed according to the 2010 American College of Rheumatology/European League Against Rheumatism classification criteria.

Isolation, culture, and differentiation of MSCs

Bone marrow–derived MSCs were isolated from the femurs and tibias of 8-wk-old male DBA/1J mice (Shanghai Laboratory Animal Center, Shanghai, China) by flushing with DMEM. Cells were centrifuged and resuspended in DMEM containing inactivated 10% FBS, 3.7 g/l HEPES, 1% L-glutamine (Life Technologies), and 1% BSA (Life Technologies). The cells were incubated at 37˚C in a humidified 5% CO_2 atmosphere for 72 h, and adherent cells were considered MSCs.

For osteogenic induction, after the cells (3×10^4 cells per well) were adhered on the plate, the osteoinductive (50 μg/ml L-ascorbic acid–2-phosphate, 10 mM glycerol 2-phosphate disodium salt, 0.1 μM dexamethasone, and 200 μg/ml rBMP-2) α-MEM medium was added, and the cells were incubated for 2 wk with medium replacement every 3 d. The cells were washed twice and stained with Von Kossa staining.

For chondrogenic differentiation, cells were cultured with chondrogenic medium (50 nM L-ascorbic acid–2-phosphate and 10 ng/ml TGF-β3). Medium was replaced every 3 d, and then the chondrogenic differentiation was stained with Alcian blue.

For adipogenic differentiation, cells were cultured with adipogenic medium (α-MEM, 10% FBS, 10 ng/ml insulin, and 1×10^{-8} M dexamethasone); cells were cultured for 3 wk with medium replaced every 3 d. Then, adipogenesis was detected by Oil Red O staining.

Flow cytometry (FCM) was used as follows: the MSCs were identified by FCM with Abs against CD105, CD90, CD73, HLA-DR, CD45, and CD31 (BD Biosciences). IgG was used as isotype control.

Culture of FLS

FLS were isolated by enzymatic digestion of synovial tissues from inflammatory arthritis patients. Briefly, tissues were harvested and collected in sterile PBS. After removal of connective tissues and fat, the tissue was digested in collagenase II in serum-free medium at 37˚C for 1 h. The cells were further dissociated by passing through a nylon mesh, and cells were collected by centrifugation at $800 \times g$ for 5 min. Cells were plated in DMEM supplemented with 10% FBS, 1% penicillin–streptomycin, and 2% L-glutamine at 37˚C in a humidified 5% CO_2 atmosphere. Cells at passages 3–6 were used for experiments.

Generation and purification of miR-150-5p exosomes

To generate miR-150-5p and miR-67 (*Caenorhabditis elegans* miR-67) as control exosomes, MSCs were transfected with locked nucleic acid–modified miR-150-5p and cel-miR-67 antisense oligonucleotides. After 48 h of miRNA transfection, exosomes were isolated from the MSCs supernatant by using an ExoQuick-TC Kit (System Biosciences) in accordance with the manufacturer's instructions. Exosome pellets were resuspended in sterile PBS at a total protein concentration 10 μg/μl, and exosome suspensions were placed on ice and administered to animals within 6 h of harvest. Exosome suspension or PBS vehicle was injected at the same coordinates using a Hamilton syringe. The severity of arthritis in each paw was measured in a blinded manner with a Plethysmometer (Marsap Services, Mumbai, India) once weekly for 4 wk.

Transmission electron microscopy and dynamic light scattering

Exosome pellets dissolved in PBS were dropped in a carbon-coated copper grid, stained with 2% uranyl acetate, and observed using a transmission electron microscope (TEM) (H7500 TEM; Hitachi, Tokyo, Japan).

The hydrodynamic sizes of the exosome pellets were measured on a Zetasizer Nano ZS (Malvern Instruments). The concentration of exosome pellets was 10 μg/ml.

Luciferase reporter assays

The MMP14 and VEGF 3′-UTRs were amplified and cloned into the XbaI site of the pGL3 vector (Promega, Madison, WI) downstream of the luciferase gene to generate the pGL3-MMP14-3′-UTR and pGL3-VEGF-3′-UTR plasmids. Mutant plasmids were generated by introducing mutations in the corresponding miR-150-5p seed sequences. Luciferase reporter assays were performed by cotransfecting FLS with 100 ng of the luciferase reporter vectors and 20 pmol of control mimic, miR-150-5p mimic, or the corresponding anti-miRs using Lipofectamine 2000 (Invitrogen). After 48 h, luciferase activity was measured using the Dual-Luciferase Assay System (Promega) and normalized to *Renilla* luciferase.

HUVEC tube formation

HUVECs were obtained from Nanjing KeyGen Biotech (Nanjing, Jiangsu, China). Tube formation assays were performed as described previously (5). HUVECs were harvested and suspended in sterile medium supplemented with 5% FBS, 100 U/ml penicillin, and 80 U/ml streptomycin. Ninety-six–well plates were prepared by coating with Matrigel, which was allowed to polymerize at 37˚C in a 5% CO_2 chamber for 30 min. HUVECs (2×10^4 cells/ml) were added to each chamber, treated as indicated, and incubated for 24 h at 37˚C in 5% CO_2, followed by imaging of capillary-like tube formation using phase-contrast microscopy.

Coculture of FLS and HUVECs

Coculture of FLS and HUVECs was performed in six-well culture plates. Proinflammatory cytokine–treated RA FLS (5×10^4 cells/ml) were seeded in DMEM supplemented with 10% FBS and allowed to adhere overnight. Cells were then washed with serum-free DMEM, and suspensions of HUVECs (ranging from 2×10^4 to 3×10^4 cells/ml) were added into the upper chamber of a transwell apparatus (CoStar Group, New York, NY). After culture in 1% FBS DMEM for 48 h, the supernatants were harvested for the subsequent tube formation assays.

Migration and invasion assays

For assessment of cell migration, FLS were plated at a density of 1×10^5 cells per chamber in serum-free DMEM in the upper chamber of transwell plates fitted with 8-μm pore membranes. DMEM supplemented with 10% FBS was added to the lower chamber as a chemoattractant. After 48 h, nonmigrating cells were removed from the upper surface and filters were stained with crystal violet. Migrated cells were counted in five representative microscopic fields at 100× magnification. For assessment of cell invasion, FLS were seeded at a density of 5×10^4 cells per chamber onto Matrigel-coated transwell plates in serum-free DMEM. The lower chamber was filled with DMEM supplemented with 10% FBS. After 48 h, cells on the top surface were removed, and invaded cells were quantified as described above.

RT-PCR

Total RNA was isolated from FLS using TriFast (Peqlab Biotechnologie, Erlangen, Germany) and reverse transcribed with random hexamers (Finnzymes, Espoo, Finland). Quantitative RT-PCR (qRT-PCR) was

performed with a DyNAmo SYBR Green qPCR kit (Finnzymes) under the following thermal conditions: 95°C for 7 min, 40 cycles of 95°C for 20 s, 60°C for 30 s, and 72°C for 15 s. GAPDH was used as a normalizing control. VEGF primers were forward, 5′-ATCCAATCGAGACCCTGGTG-3′ and reverse, 5′-ATCTCTCCTATGTGCTGGCC-3′. MMP14 primers were forward, 5′-GGCGGGTGAGGAATAACCAA-3′ and reverse, 5′-GTACTCGCTAT CCACTGCCC-3′.

Western blot analysis

Cells or tissue samples were lysed in RIPA buffer (Beyotime Biotechnology, Jiangsu, China) supplemented with protease inhibitors (Pierce), and protein concentration was determined using the BCA method (Beyotime Biotechnology, Jiangsu, China). Equal amounts of protein were separated by 10% SDS-PAGE, transferred to polyvinylidene difluoride membranes (Millipore, Bedford, MA), and blocked with 1% BSA in TBS with Tween 20 for 1 h at room temperature. Then, membranes were incubated in primary Abs overnight at 4°C, followed by incubation in the corresponding HRP-conjugated secondary Abs for 1 h at room temperature. Western bot analysis was carried out by a standard protocol using Abs for MMP14, VEGF, and GAPDH, which were from Santa Cruz Biotechnology (Santa Cruz, CA). Bands were visualized using ECL fluorography.

Animal model of CIA

Male DBA/1 mice (7–9 wk old) were obtained from Shanghai Laboratory Animal Center and kept in a temperature-controlled environment at 22°C with a 12 h:12 h light/dark cycle and fed standard chow for at least 1 wk before receiving injections. Mice were randomly divided into three groups (n = 10 per group) as follows: PBS, Exo-150, and cel-miR-67–transfected exosomes (Exo-67). CIA was induced as previously reported (15). Briefly, 150 μg bovine type II collagen (Chondrex, Redmond, WA) was dissolved in 0.01 M acetic acid overnight at 4°C and emulsified in an equal volume of CFA (Chondrex), and mice were injected intradermally at the base of the tail with 0.1-ml emulsion. Two weeks later, 150 μg type II collagen dissolved and emulsified 1:1 with IFA (Difco Laboratories) was administered to the hind leg as a booster injection. To track the exosomes that have entered the joint cavity through injection, we used immunofluorescence technology to track the exosomes labeled by DiO. Treatment was initiated after the onset of disease, when arthritis had become well established, ∼3 wk after the primary immunization. CIA mice were i.p. injected with 100 μl PBS or 100 μl PBS containing 50 μg exosomes two times per week. To monitor for arthritis, paw thickness was measured with calipers, and mice were assessed visually for arthritis severity, which was scored on a scale of 0–3 (0 = normal, 1 = slight swelling and/or erythema, 2 = pronounced swelling, and 3 = ankylosis). The results of all four limbs were added with a maximum score of 12.

Histological examination and immunohistochemistry

Joint tissues were stained with H&E, or Safranin O immunohistochemistry dye and observed at ×100 magnification. The sections were stained with H&E or Safranin O for histopathological examination.

Immunohistochemical staining of human synovium sections was performed using a streptavidin peroxidase kit. Nonspecific binding sites were blocked by incubation in a blocking solution for 30 min at room temperature. After blocking, sections were incubated in anti-MMP14 and anti-VEGF primary Abs (both Santa Cruz Biotechnology) overnight. Then, slides were washed and labeled with biotinylated secondary Abs conjugated to HRP-labeled streptavidin. Staining was visualized by diaminobenzine staining, and sections were counterstained using hematoxylin.

Statistical analysis

Data are expressed as mean ± SE. Two-way ANOVA was applied to interpret the differences between treatment groups. Differences with a p value <0.05 were considered statistically significant.

Results

Expression of miR-150-5p, MMP14, and VEGF in the serum, synovial tissue, and FLS of patients with RA

The expression of miR-150-5p, MMP14, and VEGF in serum, synovial tissue, and FLS from patients with RA was compared with that in patients with OA. The results showed that MMP14 and VEGF expression in the serum of patients was significantly higher in RA than in OA (Fig. 1A). miR-150-5p expression in the serum and synovial tissue of patients was lower in RA than in OA (Supplemental Fig. 1). qRT-PCR quantification of MMP14 and VEGF mRNA in synovial tissues showed considerably higher levels in RA than in OA (Fig. 1B). The results showed that miR-150-5p expression was significantly lower in primary FLS of RA patients than in OA (Fig. 1C), but MMP14 and VEGF expression was higher. The expression of VEGF, the angiogenesis marker CD31, and MMP14 was further determined by immunohistochemistry in sections from synovial tissues. The results showed higher staining intensity for all three markers in RA than in OA (Fig. 1D), confirming the upregulation of angiogenesis and MMP14 expression in RA.

Preparation of MSCs

We isolated mouse MSCs from bone marrow and confirmed the MSC properties of a selected clone by differentiation assay. MSCs were able to undergo multilineage differentiation when grown in specific differentiation medium. Von Kossa staining in MSCs cultured in osteogenesis differentiation medium confirms that osteogenesis has taken place (Fig. 2A). Chondrogenesis of MSCs was observed by Alcian blue staining, whereas adipogenesis of MSCs was observed by Oil Red O staining (Fig. 2C). FCM analysis with cell surface–specific markers was used to identify MSCs (Fig. 2D). MSCs were able to express CD105, CD90, and CD73 but were negative for HLA-DR, CD45, and CD31.

Exo-150 downregulated RA markers

The expression of VEGF, MMP14, and miR-150-5p was further examined in FLS (P3) from patients with OA or RA by qRT-PCR. The results showed significantly higher mRNA levels of MMP14 and VEGF and significantly lower levels of miR-150-5p in RA than in OA (Fig. 3A, 3B). MSCs were transfected with a plasmid encoding miR-150-5p or cel-miR-67 as a control, and MSC-derived exosomes were isolated from the culture supernatant. Assessment of the levels of miR-150-5p showed ∼20-fold higher miR-150-5p levels in Exo-150 than in the MSC supernatant and significantly higher miR-150-5p levels in Exo-150 than in the control Exo-67 or MSCs (Fig. 3C). There is no difference between the expression of abundant miRNAs of the exosomes of MSCs and the miRNA reported in the literature related to RA of before and after miR-150-5p–transfected MSC exosomes (Supplemental Fig. 3).These data indicate that MSCs effectively express transfected miR-150-5p in exosomes. Fig. 3D shows a representative image of MSC-derived exosomes visualized by TEM and dynamic light scattering. Because exosomes mediate the transfer of miRNAs between cells, we examined the expression of miR-150-5p in FLS incubated with Exo-150 labeled with DiO (a cell membrane green fluorescent probe) and stained with Hoechst to detect nuclei. Visualization by fluorescence microscopy showed the uptake of exosomes into FLS from patients with RA (Fig. 3E). Western blot analysis of MSC-derived exosomes showed higher expression of CD9 and the exosome marker CD63 in exosomes than in the cells (Fig. 3F). MMP14 and VEGF expression was considerably lower in Exo-150–treated RA FLS than in Exo-67–treated cells, both at the protein and mRNA levels (Fig. 3G). Taken together, these results demonstrate that miR-150-5p was successfully expressed in MSC-derived exosomes and that Exo-150 downregulated the expression of the RA markers MMP14 and VEGF in FLS.

Exo-150 inhibited migration and angiogenesis in vitro

To further examine the effect of Exo-150 on the properties of FLS, we performed migration and invasion assays comparing cells derived from OA and RA. The results showed that migration

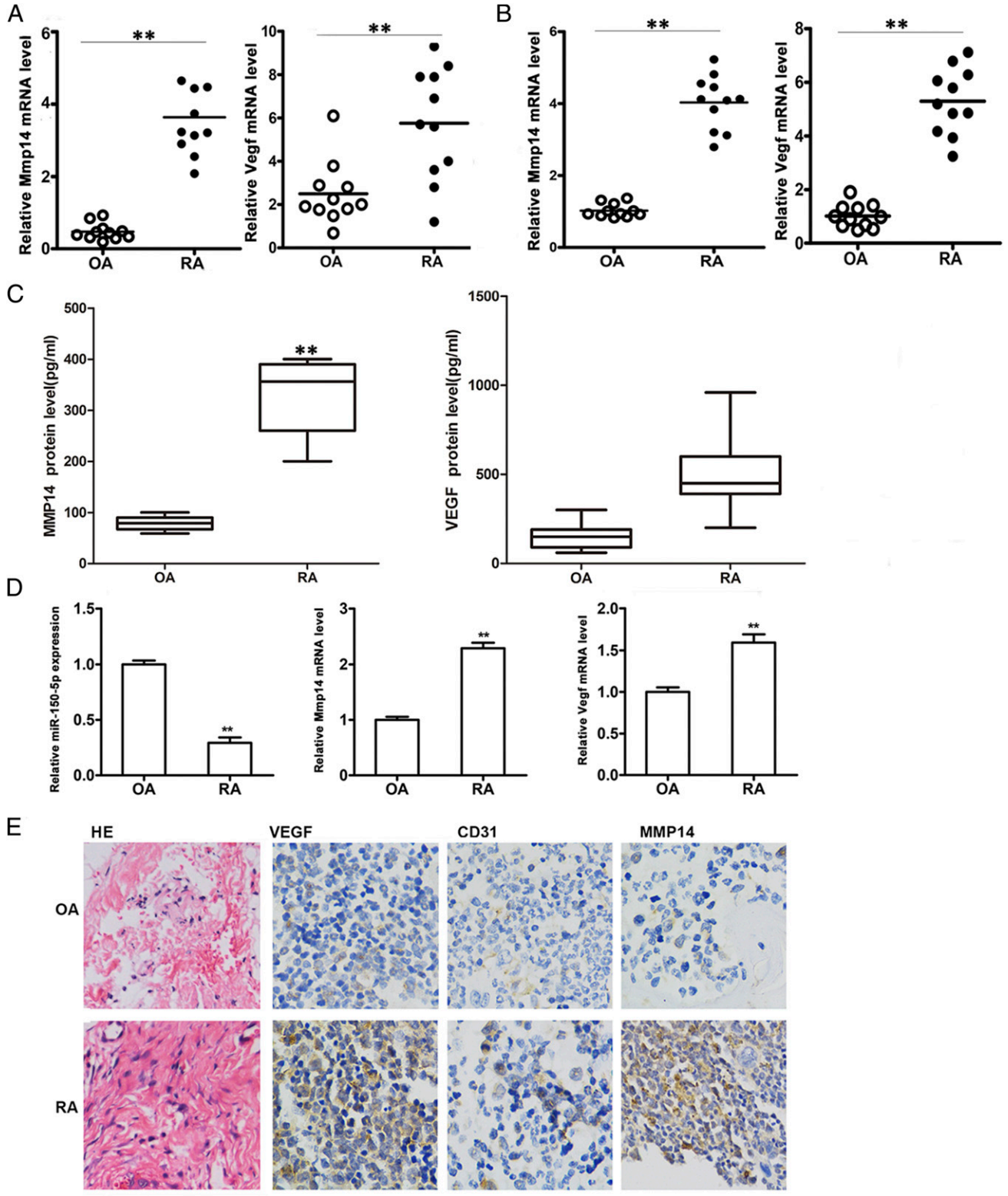

FIGURE 1. Expression of miR-150-5p, MMP14, and VEGF in the serum, synovial tissue, and FLS of patients with RA. (**A**) Quantification of *MMP14* and *VEGF* expression in serum from OA and RA patients by qRT-PCR. (**B**) *MMP14* and *VEGF* expression in OA and RA synovial tissues. (**C**) Quantification of MMP14 and VEGF protein levels in serum from of OA and RA patients by ELISA. (**D**) miR-150-5p, *MMP14*, and *VEGF* expression in OA and RA FLS cells. (**E**) Lymphocyte infiltration was analyzed using H&E (HE) staining (original magnification × 200). VEGF, MMP14, and CD31 immunohistochemistry in OA and RA synovial tissue sections (original magnification × 400). $^{**}p < 0.01$. CD31, cluster of differentiation 31.

and invasion were higher in RA than in OA FLS, and Exo-150 significantly inhibited the migration and invasion of FLS from RA (Fig. 4A). HUVEC tube formation was also significantly inhibited by Exo-150 compared with the effect of the control Exo-67, indicating the inhibition of angiogenesis by Exo-150 (Fig. 4B).

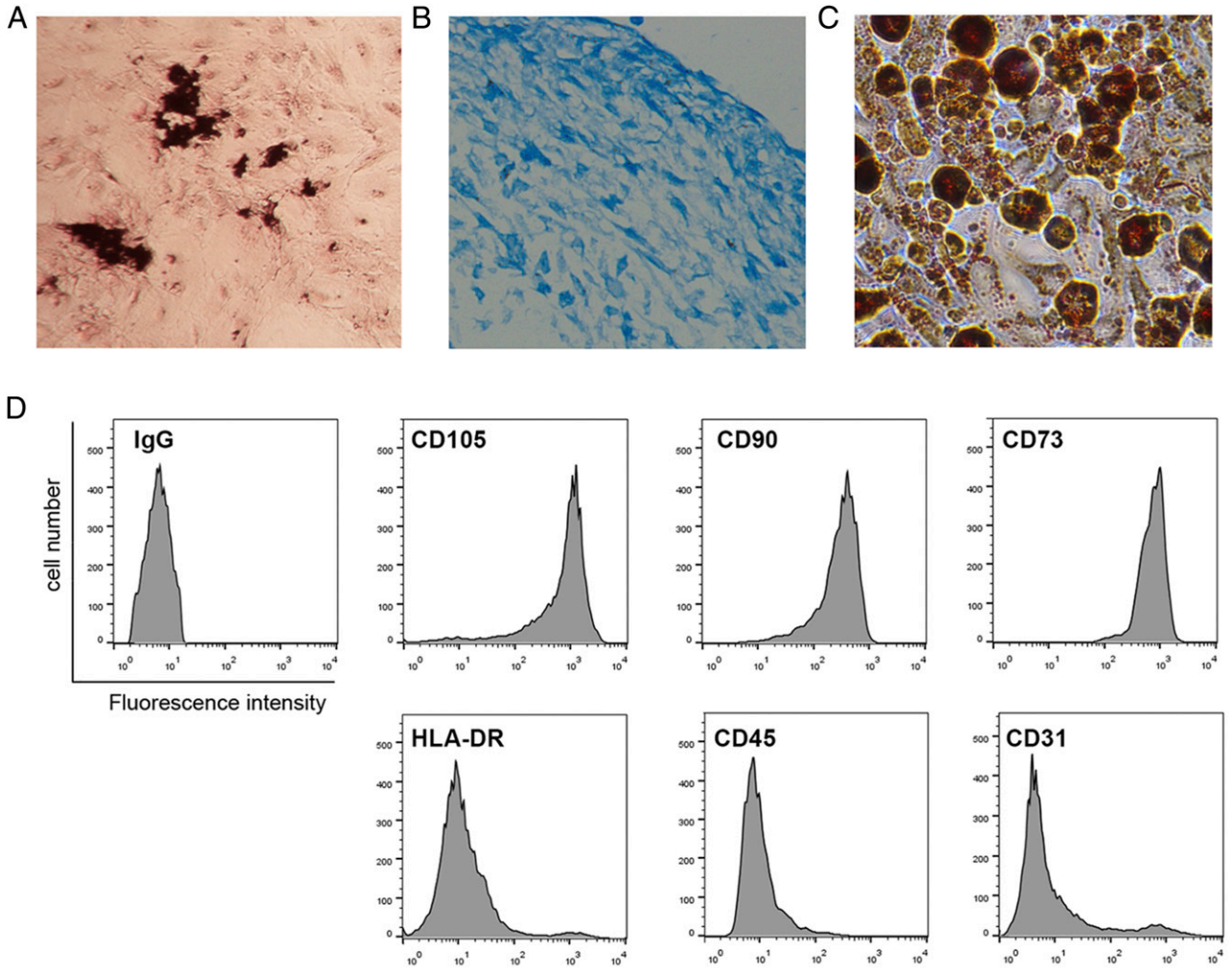

FIGURE 2. Identification of MSCs. (**A**) Von Kossa staining in MSCs cultured in osteogenic differentiation medium for 21 d. (**B**) Alcian blue staining in MSCs cultured in chondrogenesis differentiation medium for 21 d. (**C**) Oil Red O staining in MSCs cultured in adipogenesis differentiation medium for 14 d. (**D**) FCM analysis of the surface markers in MSCs.

miR-150-5p targets MMP14 and VEGF by directly binding to their 3′-UTRs in RA FLS

Fig. 5A shows the alignment of the MMP14 and VEGF 3′-UTRs and the miR-150-5p binding sites, as well as the corresponding mutant constructs generated. Luciferase assays showed that miR-150-5p significantly suppressed the transcription of the wild-type MMP14 and VEGF 3′-UTRs but not that of the mutant constructs, and miR-150-5p inhibition had the opposite effect, indicating that miR-150-5p directly targets MMP14 and VEGF and downregulates their expression (Fig. 5B). Western blot analysis showed that miR-150-5p mimics downregulated the expression of MMP14 and VEGF in FLS (Fig. 5C). qRT-PCR showed that miR-150-5p mimics downregulated MMP14 and VEGF in FLS compared with untransfected controls or miR-negative control–transfected cells, whereas transfection with anti–miR-150-5p had the opposite effect (Fig. 5D). Taken together, these results indicated that miR-150-5p downregulates MMP14 and VEGF by directly binding to their 3′-UTRs.

Effect of Exo-150 on the migration, invasion, and tube formation of proinflammatory cytokine–treated RA FLS mediated by targeting MMP14 and VEGF

To examine the anti-inflammatory effects of miR-150-5p–expressing exosomes, FLS were treated with IL-1β (5 ng/ml), TGF-β (10 ng/ml), and TNF-α (10 ng/ml), and the expression of MMP14 and VEGF as well as migration and invasion were assessed. The results showed that proinflammatory cytokines upregulated MMP14, VEGF, and miR-150-5p expression in RA FLS, whereas Exo-150 significantly abolished this effect and the control Exo-67 had no effect (Fig. 6A, 6B, Supplemental Fig. 2). Consistent with these results, Exo-150 significantly reversed the proinflammatory cytokine–induced migration (Fig. 6C) and invasion (Fig. 6D) of RA FLS, whereas Exo-67 had no effect.

We first determined the expression of VEGF in HUVECs under treatment of supernatants compared with proinflammatory cytokine–treated RA FLS from untreated RA FLS using RA FLS and HUVECs coculture system. The qRT-PCR analysis showed the expression of VEGF is significantly enhanced in supernatants of proinflammatory cytokine–treated HUVECs compared with supernatants of untreated HUVECs. Exo-150 treatment inhibited the upregulated expression of VEGF. Furthermore, we observed significantly Exo-150–inhibited HUVEC tube formation by cocultured proinflammatory cytokine–treated RA FLS and HUVEC supernatants.

Taken together, these results indicated that Exo-150 inhibited proinflammatory cytokine–induced migration, invasion, and tube formation by downregulating MMP14 and VEGF.

Exo-150 alleviated arthritis in CIA mice in vivo

To investigate the therapeutic effect of Exo-150 in vivo, CIA mice were injected with or without Exo-150 and control Exo-67, and

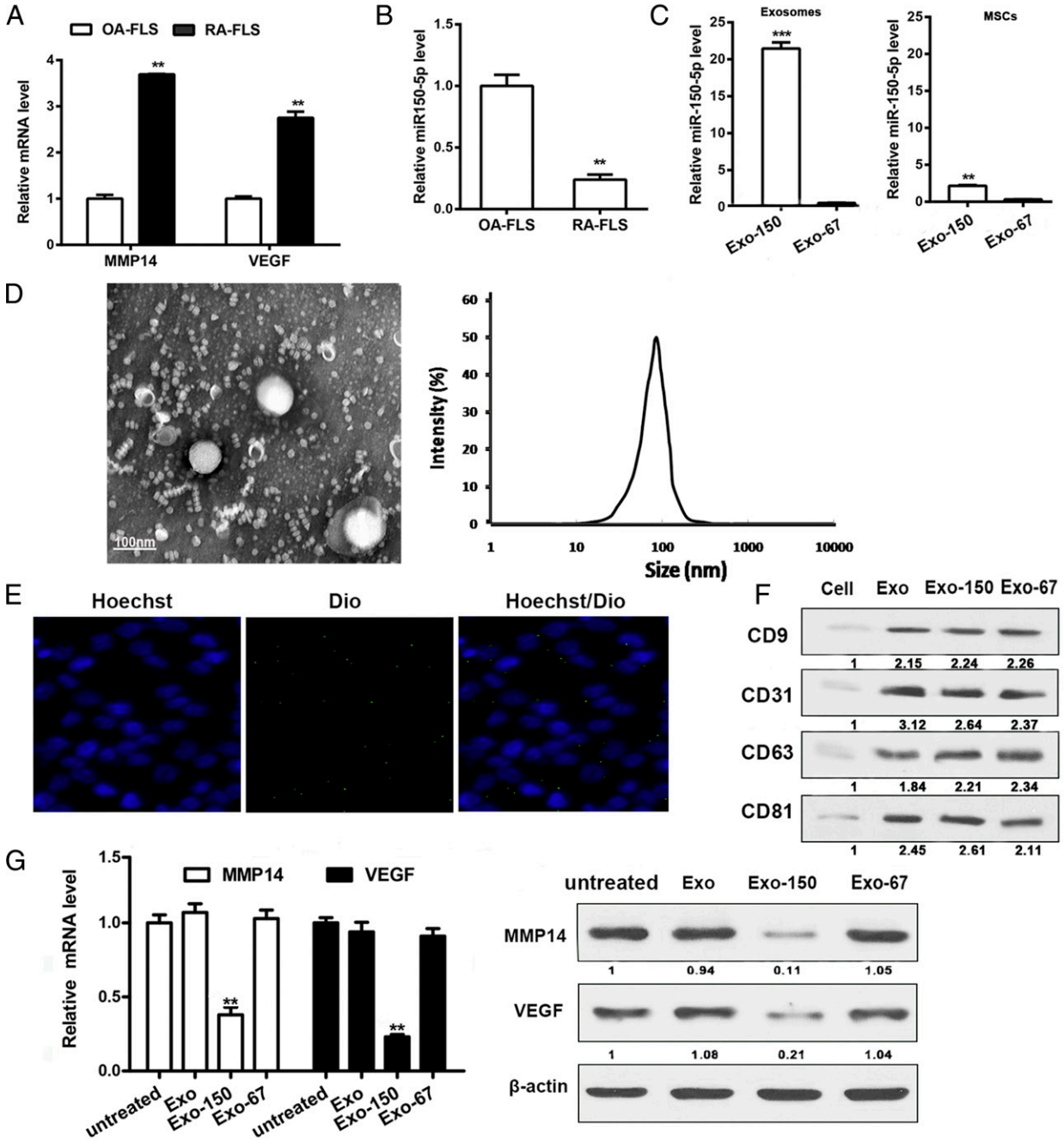

FIGURE 3. Exo-150 reduces the expression of RA markers. (**A**) *MMP14* and *VEGF* expression in OA FLS and RA FLS measured by qRT-PCR. (**B**) Endogenous miR-150-5p expression in OA FLS and RA FLS. (**C**) miR-150-5p expression in the Exo-150, Exo-67, miR-150-5p–transfected MSCs, and cel-miR-67–transfected MSCs. (**D**) Exosomes extracted from MSCs were visualized by TEM and dynamic light scattering. Scale bar, 100 nm. (**E**) RA FLS were incubated with Exo-150 and labeled with DiO. Fluorescence photomicrographs show Hoechst RA FLS nuclei (blue) and DiO-labeled exosomes (green). Merge picture shows exosome uptake into RA FLS. (**F**) Western blot showing CD9 and CD63 expression in MSC-derived exosomes. (**G**) MMP14 and VEGF mRNA expression and protein expression in Exo-150 RA FLS cells. CD63, cluster of differentiation 63; CD9, cluster of differentiation 9; MSC, adipose-derived MSC. $^{**}p < 0.01$, $^{***}p < 0.001$.

the clinical signs of arthritis were assessed. Fig. 7A showed that the exosomes came into the joint cavity, and some exosomes reach around the synovial tissue and a few enter the synovial tissue. The qRT-PCR results showed that mice treated with Exo-150 downregulated MMP14 and VEGF in tissue (Fig. 7B). Mice treated with Exo-150 showed reduced hind paw thickness and lower clinical arthritis scores compared with PBS-treated or Exo-67–treated mice (Fig. 7C, 7D). Fig. 7E shows representative histopathologic assessment of stained sections of ankle joint tissue from CIA mice on day 35. In contrast, ankle joints from the Exo-150–injected mice showed a remarkable improvement in arthritis. Immunohistochemical staining of tissue sections showed that Exo-150 reduced the staining intensity of VEGF and CD31 compared with that in PBS- or Exo-67–treated mice, indicating that Exo-150 effectively inhibited angiogenesis (Fig. 7F). Similarly, immunohistochemical staining for MMP14 and assessment of lining thickness showed that mice injected with Exo-150 had significantly lower lining thickness and reduced MMP14 expression compared with those treated with PBS or Exo-67 (Fig. 7G). These findings indicate that Exo-150 effectively downregulated MMP14 and

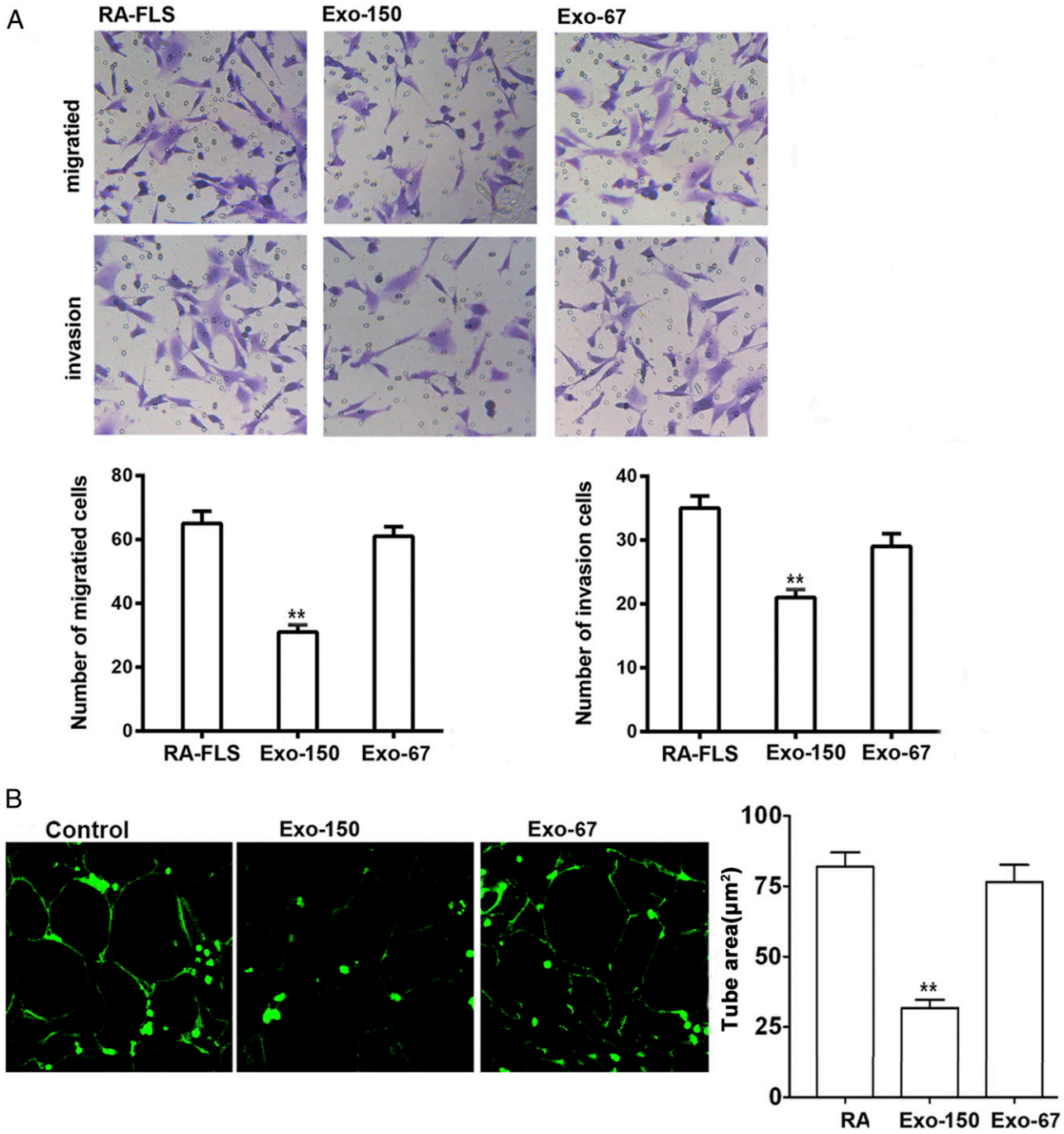

FIGURE 4. Inhibition migration and angiogenesis of by Exo-150 in vitro. (**A**) Migration and invasion assays in RA FLS cells. Administration of Exo-150 inhibited the migration and invasion of RA FLS in vitro. Original magnification ×100. (**B**) Tube formation by HUVECs was reduced by Exo-150 treatment in vitro. Original magnification ×100. $^{**}p < 0.001$.

VEGF expression, inhibited angiogenesis, and reduced the severity of arthritis in vivo.

Discussion

The ability of exosomes to shuttle small molecules between cells makes them effective therapeutic delivery vehicles and promising tools in the treatment of many diseases ranging from cancer to virus-induced and parasitic diseases (17). Furthermore, extensive research efforts have resulted in the successful manipulation of exosomal miRNAs and their delivery to target organs. Because exosomes contain cell-specific factors that mediate their selective targeting, they can efficiently deliver miRNAs to target organs or cells, making them valuable therapeutic tools. MSCs, which are increasingly being used for therapeutic purposes, are an important source of exosomes (20), and the efficacy of exosome miRNAs has been demonstrated. Approximately 150 miRNAs have been identified as part of the MSC exosome cargo, indicating their potential as therapeutic tools (29). In addition, MSC exosomes can be engineered to deliver miRNAs to specific tissues (30). Exosomes from miR-146–expressing MSCs were shown to deliver miR-146 into glioma cells in vitro and reduce the growth of glioma in a xenograft model in vivo (18). miR-122–transfected MSCs were shown to package miR-122 into exosomes and transfer the miRNA to hepatocellular carcinoma (HCC) cells, increasing the

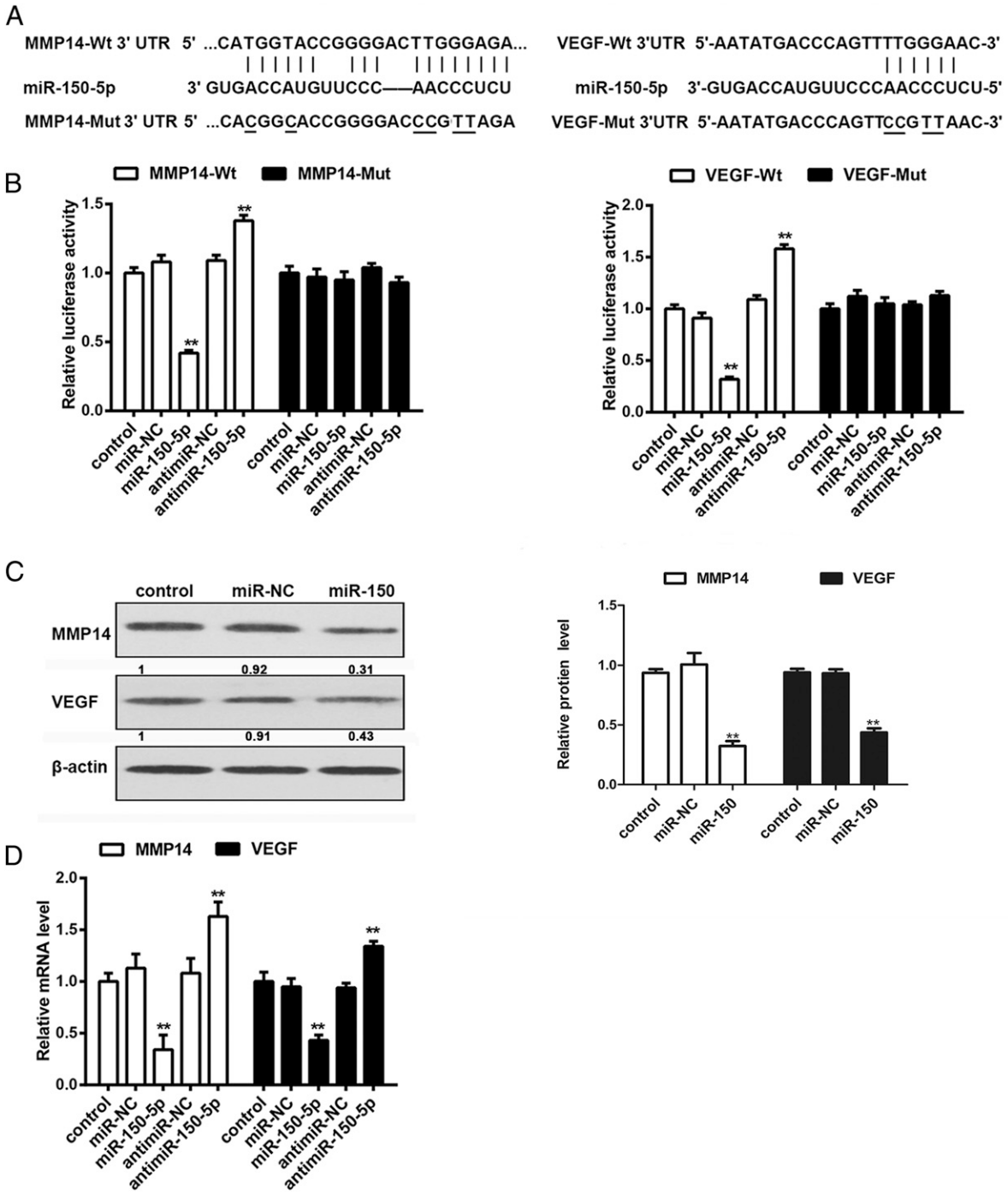

FIGURE 5. miR-150-5p suppresses *MMP14* and *VEGF* expression in RA FLS by directly binding to the 3′-UTRs. (**A**) Potential miR-150-5p binding sites on the 3′-UTR of *MMP14* and *VEGF*. (**B**) FLS were transfected with firefly luciferase reporter constructs with wild-type or mutated binding sites and miR-150-5p mimics or inhibitor, and luciferase activity was measured at 48 h after transfection. (**C**) Western blot analysis of MMP14 and VEGF protein expression in miR-150-5p–treated FLS. (**D**) qRT-PCR analysis of MMP14 and VEGF mRNA expression in miR-150-5p mimics or inhibitor-treated cells. $^{**}p < 0.001$.

chemosensitivity of HCC cells (31). Exosome-mediated transfer of miR-133b to neural cells regulates neurite outgrowth (32). In the current study, we isolated exosomes from miR-150-5p–expressing MSCs and examined the effect of these miR-150-5p exosomes on FLS from patients with RA in vitro and in a CIA mouse model in vivo.

In the current study, analysis of patients with RA and FLS from RA showed that miR-150-5p expression was significantly lower in RA than in OA, whereas VEGF and MMP14 expression and angiogenesis were increased in RA compared with OA. miR-150-5p is involved in T cell maturation and has therefore been implicated in autoimmune diseases (33). In an array-based miRNA analysis of plasma samples from patients with RA, miR-150-5p expression was lower in RA than in healthy controls (34). miR-150-5p has been shown to modulate angiogenesis and is therefore considered as a therapeutic target for the treatment of angiogenesis-related diseases (35).Furthermore, miR-150-5p overexpression inhibits cancer cell migration and invasion in HCC cells. In the current study, we showed that miR-150-5p directly targets and downregulates MMP14 and VEGF in FLS. These findings, together with the downregulation of miR-150-5p and upregulation of MMP14 and VEGF in RA, led us to hypothesize that the increased invasion and angiogenesis characteristic of RA were in part associated

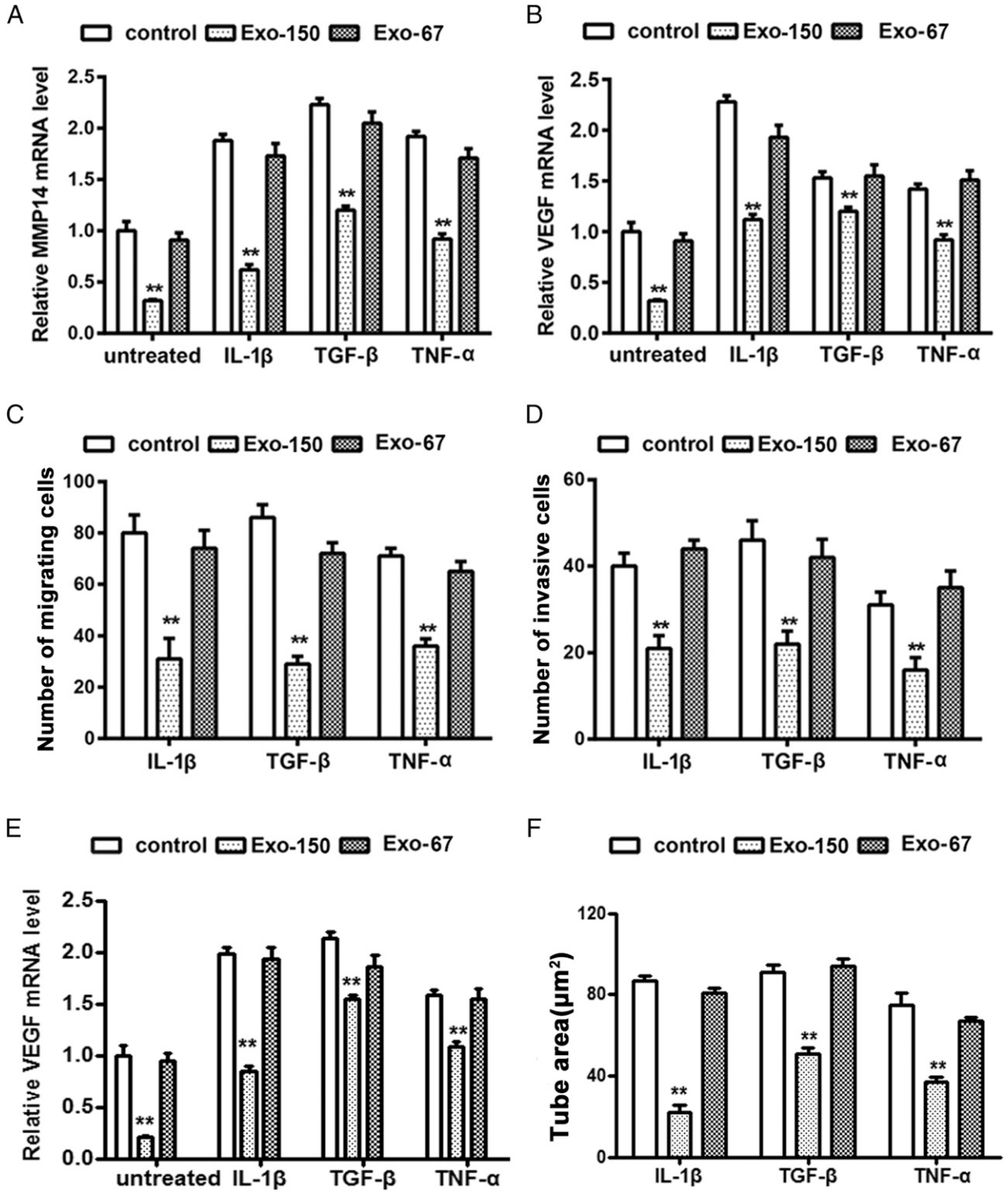

FIGURE 6. Effect of Exo-150 on the migration and invasion of proinflammatory cytokine–treated RA FLS mediated by MMP14 and VEGF. Proinflammatory cytokines upregulated *MMP14* (**A**) and *VEGF* (**B**) expression in RA FLS. The effect of Exo-150 on *MMP14* and *VEGF* expression is shown. (**C**) Effect of Exo-150 on the migration of RA FLS treated with proinflammatory cytokines. (**D**) Effect of Exo-150 on the invasion of RA FLS treated with proinflammatory cytokines. (**E**) Proinflammatory cytokines upregulated *VEGF* expression in HUVECs by cocultured RA FLS and HUVEC supernatants. (**F**) Tube formation by HUVECs was reduced by Exo-150 treatment in vitro under treatment of supernatants with proinflammatory cytokine–treated RA FLS and HUVECs coculture system. $^{**}p < 0.01$.

with the downregulation of miR-150-5p and the consequent upregulation of mediators of invasion and angiogenesis. We therefore generated Exo-150 and assessed its effect on FLS from RA patients. Our results showed that Exo-150 inhibited RA FLS migration and invasion and suppressed angiogenesis, and these effects were mediated by the downregulation of MMP14 and VEGF.

Because the articular cartilage destruction mediated by synovial inflammation is associated with the upregulation of MMPs, targeting MMPs is a potential strategy for the treatment of inflammatory joint disorders. Combined inhibition of MMP14 and TNF was shown to decrease joint damage and synovial inflammation in a CIA mouse model (36). MMPs play a role in vascular

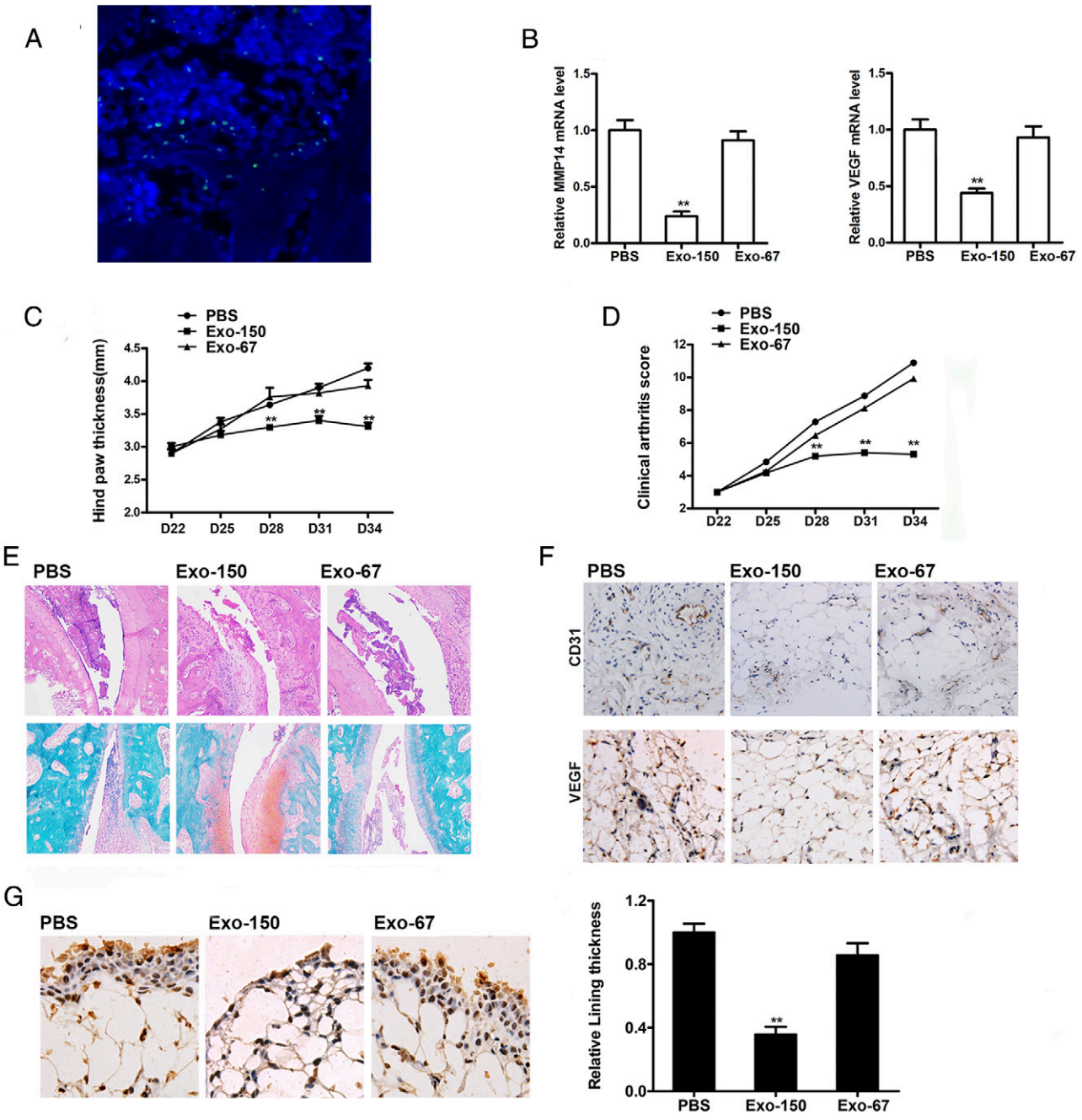

FIGURE 7. Therapeutic effect of Exo-150 in mice with established CIA. CIA mice received injection with either Exo-150 or Exo-67. (**A**) Immunofluorescence assay of DiO-labeled MSC exosomes in the CIA model articular cavity. Original magnification ×100. (**B**) Quantification of *MMP14* and *VEGF* expression in joint tissue by qRT-PCR. Hind paw thicknesses (**C**) and clinical arthritis scores (**D**) were assessed on the indicated days after primary immunization. (**E**) H&E (HE) staining and Safranin O staining of the joint tissue from CIA mice on day 35. Original magnification ×100. (**F**) VEGF and CD31 immunohistochemistry and (**G**) MMP14 immunohistochemistry of mouse synovial tissue sections prepared on day 35. Original magnification ×400. Values represent the mean and SEM of three independent experiments (n = 10 mice per group). $^{**}p < 0.01$. CD31, cluster of differentiation 31.

remodeling in part by promoting the secretion of vasoactive cytokines such as VEGF from the stromal matrix and by activating growth factors such as TGF-β (37). MMP14 acts synergistically with TGF-β to modulate vessel stability and the vascular response to tissue injury, as demonstrated by the effects of inhibition of the MMP14/TGF-β pathway on vascular stability.

Angiogenesis, which is a hallmark of RA, mediates the delivery of nutrients and inflammatory factors and activates proteases, and persistent angiogenesis can therefore lead to chronic changes in the RA synovium (5). VEGF, which is upregulated in RA and facilitates RA development, is regulated by miRNAs during angiogenesis (38, 39). miR-126 directly downregulates VEGF expression by binding to its 3′-UTR, and the RA-associated proinflammatory cytokine cysteine-rich 61 or CCN1 promotes VEGF production by inhibiting miR-126 (40). Inhibition of CCN1 alleviated joint swelling and erosion in a CIA mouse model by decreasing angiogenesis, suggesting that CCN1 is a potential target for the treatment of RA.

The results of previous studies support the targeting of VEGF and MMP14 for the treatment of RA and indicate that the modulation of miRNAs targeting these important molecules is an

effective therapeutic strategy. MSC exosomes are increasingly being used as delivery agents for therapeutic molecules, and their efficacy in promoting cartilage regeneration was recently demonstrated (27). However, further experiments are needed to verify the safety and efficacy of this approach. The use of exosomes may eliminate many of the risks associated with cell-based treatments such as the transformation of transplanted cells into cancer cells, immune rejection, and ossification/calcification (29, 41). However, their safety for the treatment of joint disorders needs to be further examined in large animal models before the application of this strategy in the clinic. We demonstrated the efficacy of Exo-150 in decreasing migration and invasion and inhibiting angiogenesis in vitro and alleviating the symptoms of RA in vivo. We showed that these effects were mediated by the downregulation of MMP14 and VEGF by exosome-delivered miR-150-5p. These results confirmed the value of MSC exosomes to mediate the direct intracellular transfer of miR-150-5p and suggested the efficacy of this strategy in RA and therefore merit further investigation.

Disclosures

The authors have no financial conflicts of interest.

References

1. Scott, D. L., F. Wolfe, and T. W. Huizinga. 2010. Rheumatoid arthritis. *Lancet* 376: 1094–1108.
2. Karsdal, M. A., S. H. Madsen, C. Christiansen, K. Henriksen, A. J. Fosang, and B. C. Sondergaard. 2008. Cartilage degradation is fully reversible in the presence of aggrecanase but not matrix metalloproteinase activity. *Arthritis Res. Ther.* 10: R63.
3. Miller, M. C., H. B. Manning, A. Jain, L. Troeberg, J. Dudhia, D. Essex, A. Sandison, M. Seiki, J. Nanchahal, H. Nagase, and Y. Itoh. 2009. Membrane type 1 matrix metalloproteinase is a crucial promoter of synovial invasion in human rheumatoid arthritis. *Arthritis Rheum.* 60: 686–697.
4. Sabeh, F., D. Fox, and S. J. Weiss. 2010. Membrane-type I matrix metalloproteinase-dependent regulation of rheumatoid arthritis synoviocyte function. *J. Immunol.* 184: 6396–6406.
5. Wang, C. H., H. Yao, L. N. Chen, J. F. Jia, L. Wang, J. Y. Dai, Z. H. Zheng, Z. N. Chen, and P. Zhu. 2012. CD147 induces angiogenesis through a vascular endothelial growth factor and hypoxia-inducible transcription factor 1α-mediated pathway in rheumatoid arthritis. *Arthritis Rheum.* 64: 1818–1827.
6. Maruotti, N., F. P. Cantatore, and D. Ribatti. 2014. Putative effects of potentially anti-angiogenic drugs in rheumatic diseases. *Eur. J. Clin. Pharmacol.* 70: 135–140.
7. Bartel, D. P. 2004. MicroRNAs: genomics, biogenesis, mechanism, and function. *Cell* 116: 281–297.
8. Bartel, D. P. 2009. MicroRNAs: target recognition and regulatory functions. *Cell* 136: 215–233.
9. Jiang, Q., Y. Wang, Y. Hao, L. Juan, M. Teng, X. Zhang, M. Li, G. Wang, and Y. Liu. 2009. miR2Disease: a manually curated database for microRNA deregulation in human disease. *Nucleic Acids Res.* 37(Database): D98–D104.
10. Niimoto, T., T. Nakasa, M. Ishikawa, A. Okuhara, B. Izumi, M. Deie, O. Suzuki, N. Adachi, and M. Ochi. 2010. MicroRNA-146a expresses in interleukin-17 producing T cells in rheumatoid arthritis patients. *BMC Musculoskelet. Disord.* 11: 209.
11. Stanczyk, J., C. Ospelt, E. Karouzakis, A. Filer, K. Raza, C. Kolling, R. Gay, C. D. Buckley, P. P. Tak, S. Gay, and D. Kyburz. 2011. Altered expression of microRNA-203 in rheumatoid arthritis synovial fibroblasts and its role in fibroblast activation. *Arthritis Rheum.* 63: 373–381.
12. Lu, M. C., C. L. Yu, H. C. Chen, H. C. Yu, H. B. Huang, and N. S. Lai. 2014. Increased miR-223 expression in T cells from patients with rheumatoid arthritis leads to decreased insulin-like growth factor-1-mediated interleukin-10 production. *Clin. Exp. Immunol.* 177: 641–651.
13. Yang, S., and Y. Yang. 2015. Downregulation of microRNA-221 decreases migration and invasion in fibroblast-like synoviocytes in rheumatoid arthritis. *Mol. Med. Rep.* 12: 2395–2401.
14. Kurowska-Stolarska, M., S. Alivernini, L. E. Ballantine, D. L. Asquith, N. L. Millar, D. S. Gilchrist, J. Reilly, M. Ierna, A. R. Fraser, B. Stolarski, et al. 2011. MicroRNA-155 as a proinflammatory regulator in clinical and experimental arthritis. *Proc. Natl. Acad. Sci. USA* 108: 11193–11198.
15. Nakasa, T., H. Shibuya, Y. Nagata, T. Niimoto, and M. Ochi. 2011. The inhibitory effect of microRNA-146a expression on bone destruction in collagen-induced arthritis. *Arthritis Rheum.* 63: 1582–1590.
16. Théry, C., M. Ostrowski, and E. Segura. 2009. Membrane vesicles as conveyors of immune responses. *Nat. Rev. Immunol.* 9: 581–593.
17. Hu, G., K. M. Drescher, and X. M. Chen. 2012. Exosomal miRNAs: biological properties and therapeutic potential. *Front. Genet.* 3: 56.
18. Katakowski, M., B. Buller, X. Zheng, Y. Lu, T. Rogers, O. Osobamiro, W. Shu, F. Jiang, and M. Chopp. 2013. Exosomes from marrow stromal cells expressing miR-146b inhibit glioma growth. *Cancer Lett.* 335: 201–204.
19. Montecalvo, A., A. T. Larregina, W. J. Shufesky, D. B. Stolz, M. L. Sullivan, J. M. Karlsson, C. J. Baty, G. A. Gibson, G. Erdos, Z. Wang, et al. 2012. Mechanism of transfer of functional microRNAs between mouse dendritic cells via exosomes. *Blood* 119: 756–766.
20. Yeo, R. W., R. C. Lai, B. Zhang, S. S. Tan, Y. Yin, B. J. Teh, and S. K. Lim. 2013. Mesenchymal stem cell: an efficient mass producer of exosomes for drug delivery. *Adv. Drug Deliv. Rev.* 65: 336–341.
21. Lai, R. C., F. Arslan, M. M. Lee, N. S. Sze, A. Choo, T. S. Chen, M. Salto-Tellez, L. Timmers, C. N. Lee, R. M. El Oakley, et al. 2010. Exosome secreted by MSC reduces myocardial ischemia/reperfusion injury. *Stem Cell Res.* 4: 214–222.
22. Hu, G. W., Q. Li, X. Niu, B. Hu, J. Liu, S. M. Zhou, S. C. Guo, H. L. Lang, C. Q. Zhang, Y. Wang, and Z. F. Deng. 2015. Exosomes secreted by human-induced pluripotent stem cell-derived mesenchymal stem cells attenuate limb ischemia by promoting angiogenesis in mice. *Stem Cell Res. Ther.* 6: 10.
23. Zhang, B., Y. Yin, R. C. Lai, S. S. Tan, A. B. Choo, and S. K. Lim. 2014. Mesenchymal stem cells secrete immunologically active exosomes. *Stem Cells Dev.* 23: 1233–1244.
24. Zhang, J., J. Guan, X. Niu, G. Hu, S. Guo, Q. Li, Z. Xie, C. Zhang, and Y. Wang. 2015. Exosomes released from human induced pluripotent stem cells-derived MSCs facilitate cutaneous wound healing by promoting collagen synthesis and angiogenesis. *J. Transl. Med.* 13: 49.
25. Zhou, Y., H. Xu, W. Xu, B. Wang, H. Wu, Y. Tao, B. Zhang, M. Wang, F. Mao, Y. Yan, et al. 2013. Exosomes released by human umbilical cord mesenchymal stem cells protect against cisplatin-induced renal oxidative stress and apoptosis in vivo and in vitro. *Stem Cell Res. Ther.* 4: 34.
26. Tan, C. Y., R. C. Lai, W. Wong, Y. Y. Dan, S. K. Lim, and H. K. Ho. 2014. Mesenchymal stem cell-derived exosomes promote hepatic regeneration in drug-induced liver injury models. *Stem Cell Res. Ther.* 5: 76.
27. Zhang, S., W. C. Chu, R. C. Lai, S. K. Lim, J. H. Hui, and W. S. Toh. 2016. Exosomes derived from human embryonic mesenchymal stem cells promote osteochondral regeneration. *Osteoarthritis Cartilage* 24: 2135–2140.
28. Qi, X., J. Zhang, H. Yuan, Z. Xu, Q. Li, X. Niu, B. Hu, Y. Wang, and X. Li. 2016. Exosomes secreted by human-induced pluripotent stem cell-derived mesenchymal stem cells repair critical-sized bone defects through enhanced angiogenesis and Osteogenesis in Osteoporotic rats. *Int. J. Biol. Sci.* 12: 836–849.
29. Toh, W. S., R. C. Lai, J. H. P. Hui, and S. K. Lim. 2017. MSC exosome as a cell-free MSC therapy for cartilage regeneration: implications for osteoarthritis treatment. *Semin. Cell Dev. Biol.* 67: 56–64.
30. Squadrito, M. L., C. Baer, F. Burdet, C. Maderna, G. D. Gilfillan, R. Lyle, M. Ibberson, and M. De Palma. 2014. Endogenous RNAs modulate microRNA sorting to exosomes and transfer to acceptor cells. *Cell Rep.* 8: 1432–1446.
31. Lou, G., X. Song, F. Yang, S. Wu, J. Wang, Z. Chen, and Y. Liu. 2015. Exosomes derived from miR-122-modified adipose tissue-derived MSCs increase chemosensitivity of hepatocellular carcinoma. *J. Hematol. Oncol.* 8: 122.
32. Xin, H., Y. Li, B. Buller, M. Katakowski, Y. Zhang, X. Wang, X. Shang, Z. G. Zhang, and M. Chopp. 2012. Exosome-mediated transfer of miR-133b from multipotent mesenchymal stromal cells to neural cells contributes to neurite outgrowth. *Stem Cells* 30: 1556–1564.
33. Ghisi, M., A. Corradin, K. Basso, C. Frasson, V. Serafin, S. Mukherjee, L. Mussolin, K. Ruggero, L. Bonanno, A. Guffanti, et al. 2011. Modulation of microRNA expression in human T-cell development: targeting of NOTCH3 by miR-150. *Blood* 117: 7053–7062.
34. Murata, K., M. Furu, H. Yoshitomi, M. Ishikawa, H. Shibuya, M. Hashimoto, Y. Imura, T. Fujii, H. Ito, T. Mimori, and S. Matsuda. 2013. Comprehensive microRNA analysis identifies miR-24 and miR-125a-5p as plasma biomarkers for rheumatoid arthritis. *PLoS One* 8: e69118.
35. Li, J., Y. Zhang, Y. Liu, X. Dai, W. Li, X. Cai, Y. Yin, Q. Wang, Y. Xue, C. Wang, et al. 2013. Microvesicle-mediated transfer of microRNA-150 from monocytes to endothelial cells promotes angiogenesis. *J. Biol. Chem.* 288: 23586–23596.
36. Kaneko, K., R. O. Williams, D. T. Dransfield, A. E. Nixon, A. Sandison, and Y. Itoh. 2016. Selective inhibition of membrane type 1 matrix metalloproteinase abrogates progression of experimental inflammatory arthritis: synergy with tumor necrosis factor blockade. *Arthritis Rheum.* 68: 521–531.
37. Sounni, N. E., K. Dehne, L. van Kempen, M. Egeblad, N. I. Affara, I. Cuevas, J. Wiesen, S. Junankar, L. Korets, J. Lee, et al. 2010. Stromal regulation of vessel stability by MMP14 and TGFbeta. *Dis. Model. Mech.* 3: 317–332.
38. Liu, G. T., Y. L. Huang, H. E. Tzeng, C. H. Tsai, S. W. Wang, and C. H. Tang. 2015. CCL5 promotes vascular endothelial growth factor expression and induces angiogenesis by down-regulating miR-199a in human chondrosarcoma cells. *Cancer Lett.* 357: 476–487.
39. Liu, S. C., S. M. Chuang, C. J. Hsu, C. H. Tsai, S. W. Wang, and C. H. Tang. 2014. CTGF increases vascular endothelial growth factor-dependent angiogenesis in human synovial fibroblasts by increasing miR-210 expression. *Cell Death Dis.* 5: e1485.
40. Chen, C. Y., C. M. Su, C. J. Hsu, C. C. Huang, S. W. Wang, S. C. Liu, W. C. Chen, L. J. Fuh, and C. H. Tang. 2017. CCN1 promotes VEGF production in Osteoblasts and induces endothelial progenitor cell angiogenesis by inhibiting miR-126 expression in rheumatoid arthritis. *J. Bone Miner. Res.* 32: 34–45.
41. Breitbach, M., T. Bostani, W. Roell, Y. Xia, O. Dewald, J. M. Nygren, J. W. Fries, K. Tiemann, H. Bohlen, J. Hescheler, et al. 2007. Potential risks of bone marrow cell transplantation into infarcted hearts. *Blood* 110: 1362–1369.